South Atlantic Ocean cyclogenesis climatology simulated by regional climate model (RegCM3)

Article *in* Climate Dynamics · December 2009

DOI: 10.1007/s00382-009-0668-7

4 authors, including:

Michelle Simões Reboita
Universidade Federal de Itajubá (UNIFEI)
118 PUBLICATIONS **1,444** CITATIONS
SEE PROFILE

Tércio Ambrizzi
University of São Paulo
196 PUBLICATIONS **7,123** CITATIONS
SEE PROFILE

Shigetoshi Sugahara
São Paulo State University
12 PUBLICATIONS **343** CITATIONS
SEE PROFILE

Clim Dyn
DOI 10.1007/s00382-009-0668-7

South Atlantic Ocean cyclogenesis climatology simulated by regional climate model (RegCM3)

Michelle Simões Reboita · Rosmeri Porfírio da Rocha · Tércio Ambrizzi · Shigetoshi Sugahara

Received: 19 March 2009 / Accepted: 10 September 2009

Abstract A detailed climatology of the cyclogenesis over the Southern Atlantic Ocean (SAO) from 1990 to 1999 and how it is simulated by the RegCM3 (Regional Climate Model) is presented here. The simulation used as initial and boundary conditions the National Centers for Environmental Prediction—Department of Energy (NCEP/DOE) reanalysis. The cyclones were identified with an automatic scheme that searches for cyclonic relative vorticity (ζ_{10}) obtained from a 10-m height wind field. All the systems with $\zeta_{10} \leq -1.5 \times 10^{-5}\ s^{-1}$ and lifetime equal or larger than 24 h were considered in the climatology. Over SAO, in 10 years were detected 2,760 and 2,787 cyclogeneses in the simulation and NCEP, respectively, with an annual mean of 276.0 ± 11.2 and 278.7 ± 11.1. This result suggests that the RegCM3 has a good skill to simulate the cyclogenesis climatology. However, the larger model underestimations (−9.8%) are found for the initially stronger systems ($\zeta_{10} \leq -2.5 \times 10^{-5}\ s^{-1}$). It was noted that over the SAO the annual cycle of the cyclogenesis depends of its initial intensity. Considering the systems initiate with $\zeta_{10} \leq -1.5 \times 10^{-5}\ s^{-1}$, the annual cycle is not well defined and the higher frequency occurs in the autumn (summer) in the NCEP (RegCM3). The stronger systems ($\zeta_{10} \leq -2.5 \times 10^{-5}\ s^{-1}$) have a well-characterized high frequency of cyclogenesis during the winter in both NCEP and RegCM3. This work confirms the existence of three cyclogenetic regions in the west sector of the SAO, near the South America east coast and shows that RegCM3 is able to reproduce the main features of these cyclogenetic areas.

Keywords Cyclogenesis · South Atlantic Ocean · Climate simulation · RegCM3

M. S. Reboita (✉) · R. P. da Rocha · T. Ambrizzi
Department of Atmospheric Sciences, Institute of Astronomy, Geophysics and Atmospheric Sciences, University of São Paulo, Rua do Matão, 1226, Cidade Universitária, São Paulo, SP 05508900, Brazil
e-mail: reboita@model.iag.usp.br

R. P. da Rocha
e-mail: rosmerir@model.iag.usp.br

T. Ambrizzi
e-mail: ambrizzi@model.iag.usp.br

S. Sugahara
Institute of Meteorological Researches and Sciences Faculty, São Paulo State University, Campus Bauru, Av. Luiz Edmundo C. Coube s/n, Vargem Limpa, Caixa Postal 281, Bauru, SP 17001-970, Brazil
e-mail: shige@ipmet.unesp.br

1 Introduction

Extratropical cyclones are formed and or intensify in some preferential regions of the globe: to the lee side of the mountains, regions of strong temperature gradients, coastal areas, etc. These systems can affect the weather over the regions where they act through cloud formation, precipitation, strong winds and temperature change (Palmén and Newton 1969). The strong winds over the ocean favor the air–sea momentum transfer that is responsible for the ocean disturbance which may lead to the occurrence of the high sea waves causing problems to the navigation, petroleum platforms, and severe shore erosion. On the other hand, extratropical cyclones have a central role on the global climate equilibrium, acting in large proportion in the atmosphere heat, water vapor and momentum transport towards the poles (Peixoto and Oort 1992). Therefore, a better acknowledge of the behavior of these systems in terms of their formation, frequency, trajectory and intensity

Published online: 23 September 2009

may be useful for their prediction, minimizing economic loss or even lives.

Climatological studies of extratropical cyclones over South America and adjacent oceans have been done by many authors using different methodologies to identify and tracking these systems. Necco (1982a, b) identified the systems using near surface streamlines analysis and Gan and Rao (1991) using minimum mean sea level pressure (MSLP) over synoptic charts; Satyamurty et al. (1990) identifying vortices in satellite images; Sinclair (1996) and Reboita et al. (2005) have used cyclonic relative vorticity from global reanalysis. Gan and Rao (1991) found two preferential regions of cyclogenesis over the east coast of South America: one on the southeastern coast of Argentina ($\sim$42°S), and other in the Uruguay coast. Some other authors (i.e. Sinclair 1996; Hoskins and Hodges 2005) also found large occurrence of systems on the south/southeastern coast of Brazil ($\sim$25°S).

There have been many studies (Lambert 1988, 1995; Murray and Simmonds 1991; König et al. 1993; Hodges 1994, 1996) performing cyclone tracking in simulations of the present climate using atmospheric global circulation models (GCM) in order to verify their skill once synoptic systems involve complex interactions with different spatial and temporal scales, being an efficient way to validate them (Sinclair and Watterson 1999). Other authors (Zhang and Wang 1997; Hudson and Hewitson 1997; Hudson 1997; Blender et al. 1997; Sinclair and Watterson 1999; Fyfe 2003; Raible and Blender 2004; Watterson 2006) have investigated the cyclone climatology in GCM simulations of future climate considering the increase of the greenhouse gases (IPCC 2007).

A fundamental issue concerning the use of GCM to provide regional climate scenarios is about horizontal resolution. GCM are still run at horizontal grid intervals of 100–300 km. While this resolution is sufficient to capture the large scale processes of the climate (Giorgi and Mearns 1991), it is not suitable for finer regional and local scales. One alternative to that was originally proposed by Dickinson et al. (1989) and Giorgi (1990). They suggested to use limited area models or as it is known nowadays, Regional Climate Models (RCM). This idea was based on the concept of one way nesting, in which large scale meteorological fields from GCM runs provide initial and time-dependent meteorological lateral boundary conditions for RCM simulations.

Many previous studies have already used RCM to simulate some climate features over South America (Seth and Rojas 2003; Fernandez et al. 2006; Pal et al. 2007), but most of them were not concerned about extratropical cyclonic systems and how skillful the RCM are to simulate their climatology. More recently, Lionello et al. (2008) analyzed the cyclone climatology over Europa, using the RegCM3 to simulate the present (1961–1990) and future climate (2071–2100). When compared to the European Centre of Medium Range Weather Forecasting (ECMWF; Uppala et al. 2005) reanalysis data the RegCM3 was able to reproduce the main cyclones climatological features, particularly their spatial distribution.

The main objective of this study is to evaluate the ability of the RegCM3 in simulate the cyclone climatology on the large part of South Atlantic Ocean (between 15° and 55°S) in the period 1990–1999. Knowing the strength and limitations of the RegCM3 to simulate the present climate is important if one wants to use this model in projections of future climate scenarios. This paper is organized as follow: Sect. 2 briefly describes the RegCM3, the simulation main features, data used, the cyclone tracking scheme and the analysis to be done. The results are presented in Sect. 3 and some concluding remarks are given in Sect. 4.

2 Regional model, data and methodology

2.1 RegCM3 description

The RegCM3 limited area model has the dynamical core based on the hydrostatic version of the National Center for Atmospheric Research-Pennsylvania State University (NCAR-PSU) Mesoscale Model version 5 (Pal et al. 2007). RegCM3 is a primitive equation, compressible and in sigma-pressure vertical coordinate model.

The RegCM3 surface physics processes are obtained using the Biosphere–Atmosphere Transfer Scheme (BATS version 1e, Dickinson et al. 1993). This scheme describes the role of the vegetation (or water) in the modification of the moment, energy and water vapor fluxes exchange between surface and atmosphere. In the formulation of the planetary boundary layer, the turbulent transport of energy, moment, and moisture results from the product between their vertical gradient and the coefficient of turbulent vertical diffusion, with a non-local turbulent formulation proposed by Holtslag et al. (1990). Over the ocean the surface turbulent fluxes can be calculated following Zeng et al. (1998), where the roughness length is a function of the atmospheric stability and near surface wind intensity. The NCAR CCM3 (Community Climate Model 3; Kiehl et al. 1996) radiative transfer scheme is used in the RegCM3. The precipitation is represented in two forms: grid-scale (resolvable scale) and convective (subgrid-scale). The grid-scale precipitation scheme (Pal et al. 2000) only considers the water phase and includes formulations for auto-conversion of cloud water into rainwater, accretion of cloud droplets by falling raindrops, and evaporation of falling raindrops. Three options are available to represent cumulus convection: (1) the modified Anthes-Kuo scheme

(Anthes 1977; Giorgi 1991); (2) the Grell scheme (Grell 1993); and (3) the Massachusetts Institute of Technology (MIT) scheme (Emanuel 1991).

2.2 Numerical simulation and data

The simulation domain includes large part of the South Atlantic Ocean (SAO) and most part of South America, from 5°–60°S to 84°W–15°E, as shown in Fig. 1. The simulation is initiated in September 1989 and finished in January 2000. The three-first months of the integration were considered as spin-up time. The model was integrated with a resolution of 60 km in the horizontal, 18 vertical sigma-levels, Zeng scheme for ocean fluxes parameterization and the Grell scheme with the Fritsch–Chappell closure to solve the convective precipitation.

Reanalysis of the R2 project (Kanamitsu et al. 2002) of the National Center for Environmental Prediction—Department of Energy (NCEP-DOE, hereafter NCEP) provided the variables (relative humidity, geopotential height, air temperature, meridional and zonal wind, and surface pressure) for initial and boundary conditions of the simulation. These data are available four times a day (00:00, 06:00, 12:00 and 18:00 UTC) with horizontal resolution of 2.5° and 17 vertical pressure levels. The topography and land cover data were obtained from the global archives (horizontal resolution of 10′) derived from the United States Geological Survey (USGS) and Global Land Cover Characterization (GLCC, Loveland et al. 2000), respectively. The sea surface temperature (SST) dataset was specified using the Reconstructed SST developed by Reynolds et al. (2002), which is a global field with horizontal resolution of 1°.

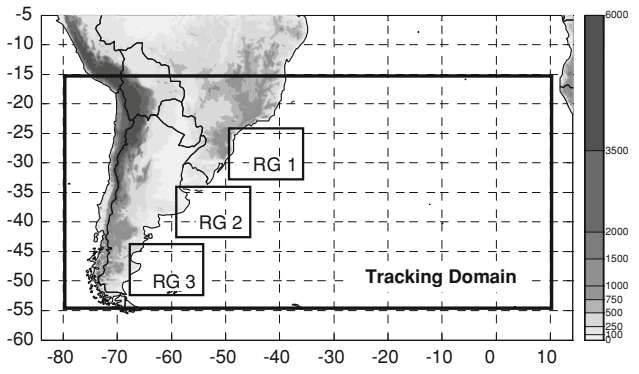

Fig. 1 Simulation domain (total area, from 84°W–15°E to 60–5°S), tracking domain (*inner big rectangle*) and the three regions (*RG1*, *RG2* and *RG3*) used to analyze the cyclogenetic activity on the South American coast. The topography of the South America is also indicated (*shaded*)

2.3 Cyclone tracking algorithm

The algorithm initially developed by Sugahara (2000) for tracking the extratropical cyclones was modified in order to be applied in the present work. The methodologies of this algorithm are similar to those used by Sinclair (1994, 1995 and 1997) where cyclones are identified using cyclonic relative vorticity from near surface wind. One advantage to use vorticity compared to pressure minimum is that as vorticity measures the fluid rotation it can identify more accurately the cyclonic systems (Sinclair 1994). This eliminates the common problem of algorithms which use pressure minimum that produces less cyclonic systems in middle latitudes. In this region, the intense meridional gradient of pressure, superimposed over the cyclonic circulation, many times imply in cyclones that do not have closed isobars and they are not identified by automatic procedures based on pressure minimum. Some disadvantages of the vorticity algorithm are: it is sensitive to analysis errors (errors in the wind measured imply on errors in the vorticity); the intensity of the vorticity is a function of the horizontal resolution of the analysis; and the inclusion of vorticity centers in elongated shear regions, which can not be associated to typical cyclonic structure.

In the present algorithm, the cyclones were identified in the vorticity field obtained from 10 m height wind calculated as:

$$\zeta_{10} = \frac{\partial v_{10}}{\partial x} - \frac{\partial u_{10}}{\partial y}$$

which is resolved numerically using the finite differences method centered in the space.

Before starting the cyclones tracking the vorticity field is smoothed with the Cressman method (Cressman 1959) to eliminate spurious vorticity centers and to reduce noises elongated shear regions (Sinclair 1997). The cyclones tracking process basically involves three stages: (1) minimum vorticity identification, (2) locating of the position after the first displacement, and (3) search for the next positions considering the estimate of cyclone velocity.

The first stage identifies the cyclonic vorticity minimum through of the *nearest-neighbor search*, i.e., the vorticity in each grid point is compared with the 24 nearest points. A grid point is considered a cyclone center when the vorticity is the lowest among its neighbors and it is lower than a threshold previously established. Once the cyclone center is located, the ζ_{10} field around it is interpolated (using bicubic spline) to a higher resolution grid, where the vorticity minimum is searched again. This procedure can produce a difference in the position of the cyclone center of about 100 km (Sugahara 2000). The position obtained after this correction is considered the cyclone center.

A cyclone trajectory is defined as a sequence of its position in the time $\{x(t), y(t)\}$ and the system lifetime is obtained from its first identification up to its disappearance. After identify the cyclone first position (stage 1) is necessary to identify its position after the first displacement (stage 2) and the next positions (stage 3). As in Sinclair (1994) the cyclone trajectory is performed to match cyclones at the current time t with the centers obtained for the following analysis time $t + \Delta t$. In the stage 2, the cyclone localization obtained in the stage 1 is used to search the new cyclone center position by comparing with the *nearest-neighbor* points, i.e., the first position is repeated in the following time ($t + \Delta t$) and there is a search by vorticity minimum in the 24 grid points around. Once the position of the system between two consecutive time intervals is known the cyclone speed is calculated. This velocity is used to estimate the new position in the next time step (stage 3). After the identification of this probable position of the system center, the algorithm searches again the vorticity minimum in the 24 grid points around. Future positions are determined considering the estimative of cyclone velocity between the two consecutive time intervals and cyclonic vorticity threshold. In the stages 2 and 3 the position of the cyclone center is also corrected in a high resolution grid. The end of the cyclone occurs when both the vorticity minimum and its lifetime overcome the thresholds previously established.

At each time step the vorticity minima are considered as new cyclone. This results in many trajectories for the same system. After all tracking a filter is used to eliminate the trajectories that have a minimum of three repeatedly positions and times. Sometimes two systems starting in different places can join, assuming similar positions during part of their lifetime. If this happens, in order to not allow the filter to eliminate the last system it is necessary to verify if it has at least five different positions before. In this case the second system is not eliminated by filter.

The final result of the algorithm supplies the cyclone center position (latitude and longitude), date, pressure and its ζ_{10}.

2.4 Analysis methods

The 10-m height wind field with 6-h-temporal resolution obtained from the NCEP and the RegCM3 are originally in a gaussian grid and Mercator projection, respectively. For the cyclones tracking, the bi-linear interpolation scheme was used to construct a 2.5° × 2.5° regular grid. The objective was to guarantee that we are seeking the same type of system in the RegCM3 and in the NCEP. It is known that vorticity is very dependent of the grid resolution; however, the frequency and intensity of the cyclones are also sensitive to that (Pinto et al. 2006). Adopting the same low resolution grid is a procedure that filters small scale cyclogenesis of the RegCM3 higher resolution and also does not create unrealistic cyclones that could result from the interpolation of NCEP to RegCM3 grid.

The tracking algorithm compares the vorticity values with the 24 nearest grid points. The adopted thresholds for cyclone identification were: (a) $\zeta_{10} \leq -1.5 \times 10^{-5}$ s^{-1}, (b) T ≥ 24 h, where T is the cyclone lifetime; (c) $T \leq 10$ days. The period of study is from January 1, 1990 to December 31, 1999. The cyclones tracking area is shown in Fig. 1 and in the analyses of the results it was only considered the systems that initiated over SAO. It is important to mention that the methodology used identifies vorticity minima associated with isobars open or closed.

A validation of the tracking algorithm was done by comparing the vorticity fields (simulated and reanalysis) and cyclone centers identified by the algorithm for several months. It was found that the algorithm correctly tracks most of the relative vorticity minima, i. e., the algorithm is able to capture between 85 and 95% of the systems identified in the vorticity field.

The occurrence of cyclogenesis in the NCEP and RegCM3 was investigated through annual, seasonal and monthly means in the analysis domain (Fig. 1) and in three subdomains shown in the Fig. 1 (RG1, RG2 and RG3). These areas were chosen due the higher frequency of cyclogenesis over the east coast of South America (Necco 1982a, b; Satyamurty et al. 1990; Gan and Rao 1991; Sinclair 1996; Hoskins and Hodges 2005, and Reboita et al. 2005) and represent the south/southeastern coast of Brazil (RG1), the La Plata River discharge in Uruguay (RG2) and southeastern coast of Argentina (RG3). The cyclogenesis geographical distribution was analyzed by calculating the mean density that is the number of systems in a 5° × 5° region divided by the same area. This procedure follows Murray and Simmonds (1991) and to facility the results presentation the mean density was multiplied by 10^4 in the figures.

3 Results: cyclogenesis climatology

3.1 Subjective comparison: NCEP × RegCM3

The comparison between the cyclones obtained from the NCEP and those simulated by the RegCM3 shows that the later has a tendency to start 12–24 h after those NCEP. However, in general the simulated systems tend to decay after the observed ones. Therefore this implies in a similar cyclone lifetime for the NCEP and RegCM3.

Cyclogeneses monthly frequency over SAO, in general, shows a little difference between NCEP and RegCM3.

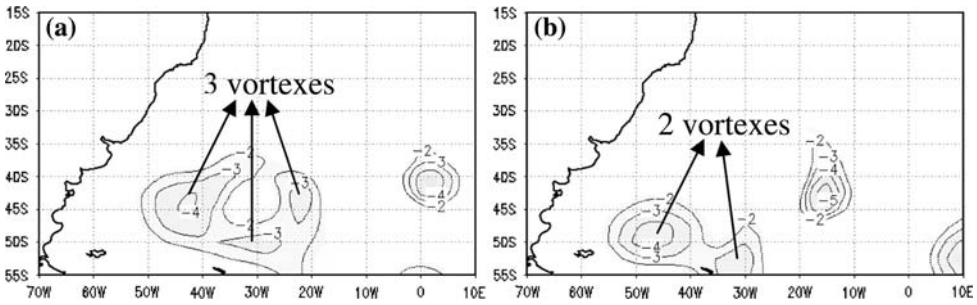

Fig. 2 Comparison between the smoothed relative vorticity ($\zeta \leq -1.5 \times 10^{-5}$ s^{-1}) of the **a** NCEP reanalysis and **b** RegCM3 simulation (*right*) in June 25, 1996 at 12 UTC

Several factors can be responsible for it. For example, some systems that developed in the study area, mainly near the south/southeastern coast of Brazil, can have a lifetime below 24-h in the simulation and higher in the NCEP, therefore, the first one are excluded of the statistics, once it does not satisfy the algorithm lifetime threshold. Other situation is when the systems leave the study area before it reaches the 24 h lifetime in NCEP or RegCM3. An additional factor that also contributes to the differences in the climatology is the cyclonic vortices that are close to each other (Fig. 2). Sometimes several vorticity centers occur within a single complex low pressure area, though with similar pressure, these centers often have widely varying vorticity. For this, they require an individual tracking (Sinclair 1994). This pattern is more frequently found in the NCEP than in the RegCM3 fields. In general, the subjective analysis demonstrated that in the monthly average these situations occur about three to five times which could explain the differences found between the simulation and the NCEP.

3.2 Interannual variability

For the analysis domain (see Fig. 1), Fig. 3a and b presents the total annual of cyclogenesis that initially have $\zeta_{10} \leq -1.5 \times 10^{-5}$ s^{-1}, hereafter $\zeta_{-1.5}$, and $\zeta_{10} \leq -2.5 \times 10^{-5}$ s^{-1}, hereafter $\zeta_{-2.5}$, respectively. It is important to note that the number of cyclones initiated with $\zeta_{-1.5}$ includes those initiated with $\zeta_{-2.5}$. Figure 3a shows that the interannual variability of the cyclogenesis initiated with $\zeta_{-1.5}$ in the RegCM3 is similar of the NCEP, with some exceptions in the firsts three years and in 1997, when the two series have inverse behavior. In absolute value the RegCM3 and NCEP show small differences (maximum 29 systems in 1990), but the RegCM3 tend to underestimates the cyclogenesis number (Fig. 3a). During the 10 years, the total of cyclogenesis initiated with $\zeta_{-1.5}$ is 2,760 in RegCM3 and 2,787 in NCEP, which corresponds to the annual mean and standard deviation of the 276.0 ± 11.2 and 278.7 ± 11.1, respectively. This implies that in mean the RegCM3 has an underestimation of only −1% of the systems by year. In 1990, 1992, 1993 and 1995 the RegCM3 overestimates the cyclogenesis (Fig. 3a), where in first two years it was 11.1 and 3.7%, respectively.

Considering the vorticity threshold $\zeta_{-2.5}$, where the cyclones are initially more intense (Fig. 3b), the interannual variability simulated by RegCM3 shows some differences in relation to the NCEP in the years of 1991, 1992, 1994 e 1996. It is also observed that there is an increase of the RegCM3 underestimates when compared with the cyclogenesis of $\zeta_{-1.5}$ threshold (Fig. 3a, b). For the 10-years period it was identified a total of 948 and 1,047 cyclogenesis started with $\zeta_{-2.5}$ in the RegCM3 and NCEP, respectively. This provides an annual mean and standard deviations of 94.8 ± 9.8 for the RegCM3 and 104.7 ± 14.3 for NCEP, implying in a difference of −9.5% systems by year in the RegCM3 climatology. This result indicates that the model underestimates the cyclones that are more intense at the beginning of their formation and also their interannual variability.

Figure 3a can be compared with Fig. 6a from Simmonds and Keay (2000), who studied the extratropical cyclones variability in the NCEP-NCAR reanalyses (Kalnay et al. 1996) between 1958 and 1997. Although these authors used different methodology in the cyclones identification (e.g., mean sea level pressure minima) and include all South Hemisphere in their analysis, the interannual variability from 1990 to 1997 is similar to that obtained in the present study for NCEP-DOE (Fig. 3a). This also indicates that the algorithm is tracking similar systems to those using pressure minima.

The interannual variability of the systems that initiated with different vorticity thresholds is presented in Fig. 4. It can be noted that the number of weak systems ($-2.5 < \zeta \leq -1.5$, Fig. 4a) is larger in the RegCM3 than in the NCEP, while the model underestimates the more intense ones ($\zeta \leq -3.5$, Fig. 4c). However, in both thresholds the simulated interannual variability is similar to the NCEP. With relations to the systems with intermediary initial vorticity (Fig. 4b), in some years the model presents a reversed pattern when compared to the NCEP; however, in absolute values the differences are small. For the period showed in Fig. 4a, the RegCM3 (Table 1) simulates 4.1% initially weak systems above the NCEP and 2.9% below for

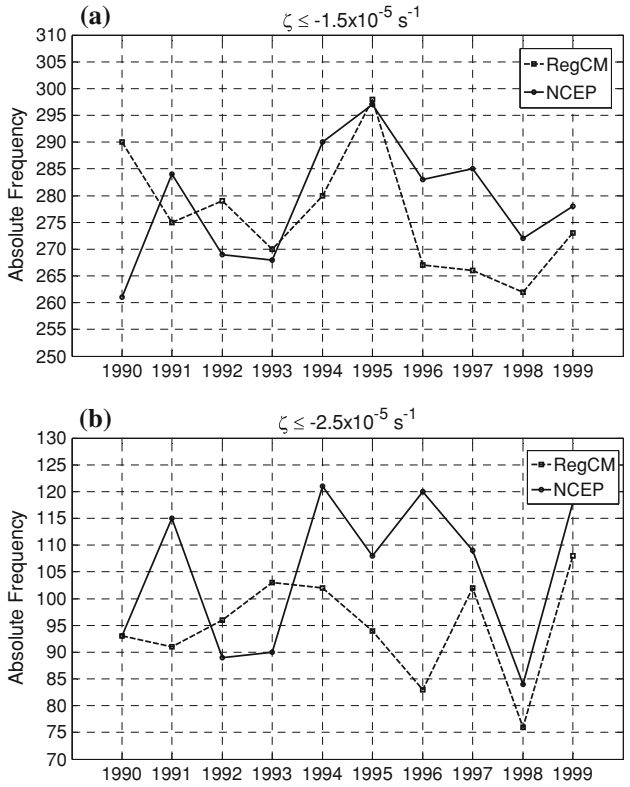

Fig. 3 Annual cyclogeneses occurrence in the SAO from 1990 to 1999 detected in the simulation (*dotted line*) and NCEP (*full line*): **a** with $\zeta_{-1.5}$ and **b** with $\zeta_{-2.5}$

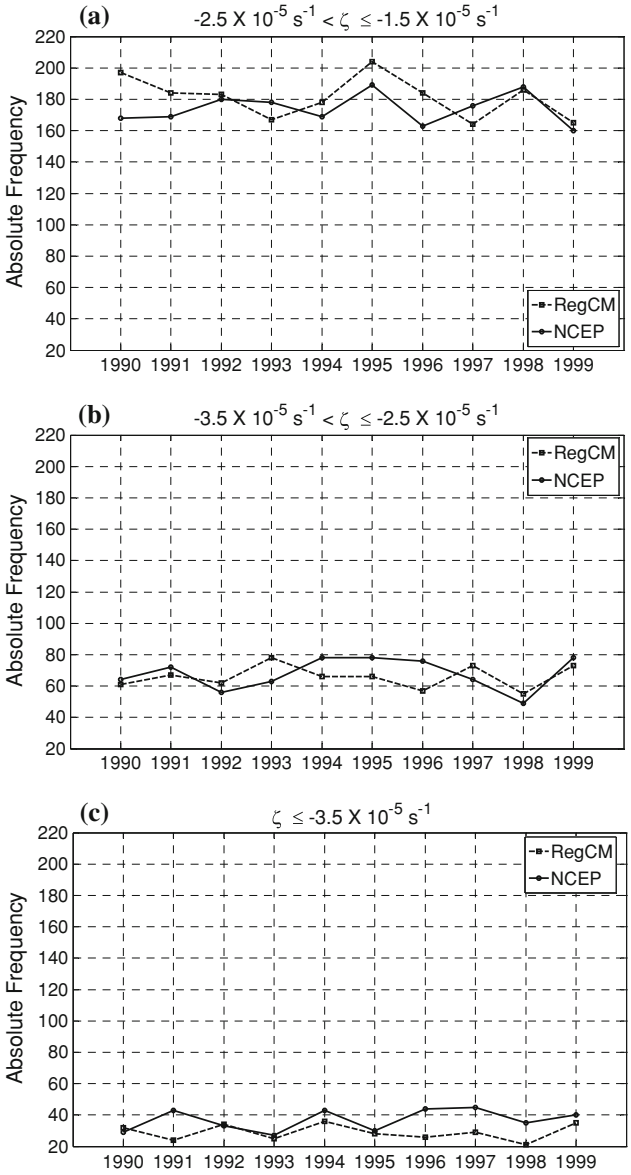

Fig. 4 Annual total of cyclogeneses that started at different vorticity intervals: **a** $-2.5 \times 10^{-5}\ s^{-1} < \zeta \leq -1.5 \times 10^{-5}\ s^{-1}$; **b** $-3.5 \times 10^{-5}\ s^{-1} < \zeta \leq -2.5 \times 10^{-5}\ s^{-1}$; **c** $\zeta \leq -3.5 \times 10^{-5}\ s^{-1}$

the intermediate ones. The larger underestimation is 21.4% for the initially stronger systems (Table 1).

3.3 Annual cycle

The annual cycles of the all cyclogenesis ($\zeta_{-1.5}$) and initially intense ($\zeta_{-2.5}$), are presented in Fig. 5. For $\zeta_{-1.5}$ systems, the monthly variability simulated by the RegCM3 is similar to the NCEP (Fig. 5a), and in both the annual cycle is not properly defined. In this case the maxima cyclogenesis is not obtained in the winter, which was also noticed by Sinclair (1996). In the NCEP the larger number of events (Fig. 5a) is obtained during May (~27.6), the same month that the RegCM3 simulates high frequency of systems (~25.5). However, in absolute values the RegCM3 highest frequency occurs in December (~26.3). The cyclogeneses maximum in May was also obtained by Gan and Rao (1991) who used sea level pressure maps to identify these systems. February, April and November are the months with lower occurrence of cyclones in the NCEP and in the RegCM3 (Fig. 5a). Figure 5a also shows that the monthly variability of systems with $\zeta_{-1.5}$ presents small amplitude. This feature agrees with Sinclair (1996).

Considering the cyclones initiated with $\zeta_{-2.5}$, it is noticed from Fig. 5b a well defined annual cycle with large number of systems during the winter and small in the summer months. In monthly scale, both NCEP and RegCM3 show maximum and minimum of cyclogenesis in June and February/November, respectively. In general, the RegCM3 underestimates by about 0.5–1.0 cyclogenesis per month when compared to the NCEP, but in June and October the underestimation is almost double (Fig. 5b).

Section 3.1 discussed the possible causes of the differences in the number of cyclogenesis between RegCM3 and NCEP, where it was mentioned that, per month, a difference of ~3–5 systems can occur between the climatologies. For further emphasize this difference, Fig. 6 presents the monthly differences between the RegCM3 and NCEP

Table 1 Total number of cyclogeneses that started with different vorticity threshold in the RegCM3 and NCEP and the relative bias (RegCM3-NCEP)

Thresholds $\zeta \times 10^{-5}$ s^{-1}	RegCM3	NCEP	Relative bias (%)
$-2.5 < \zeta \leq -1.5$	1,812 (65.7%)	1,740 (62.5%)	4.1
$-3.5 < \zeta \leq -2.5$	658 (23.8%)	678 (24.3%)	−2.9
$\zeta \leq -3.5$	290 (10.5%)	369 (13.2%)	−21.4

Values in parenthesis are percentage of cyclogeneses in each interval in relation the total of systems identified

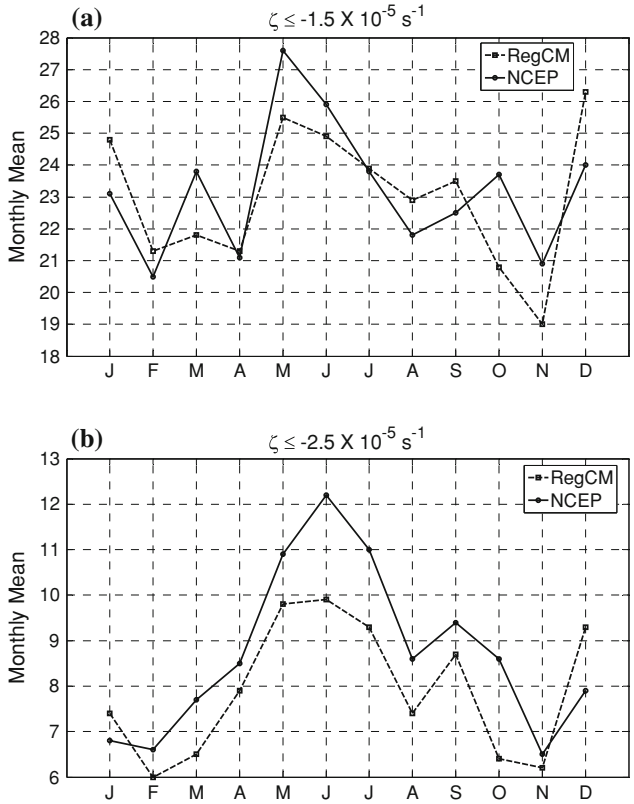

Fig. 5 Monthly mean cyclogeneses detected from NCEP (*full line*) and simulated by the RegCM3 (*dotted line*) with initial vorticity: **a** $\zeta \leq -1.5 \times 10^{-5}$ s^{-1} and **b** $\zeta \leq -2.5 \times 10^{-5}$ s^{-1}

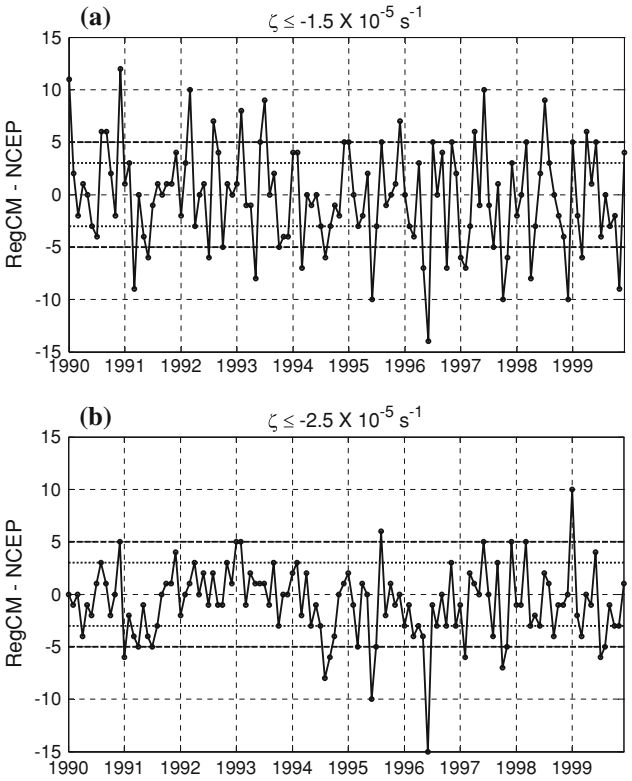

Fig. 6 Difference between RegCM3 and NCEP (RegCM3-NCEP) of the monthly number of cyclogeneses detected for the systems with **a** $\zeta_{-1.5}$ and **b** $\zeta_{-2.5}$. The *dotted line* indicates the threshold of the ±5 systems and the *dashed line* ±3 systems

in the number of cyclogenesis detected and Table 2 depicts the number of months in which this difference exceeded the threshold of ±3 and ±5 systems per month. The differences, absolute and relative (Table 2), between the RegCM3 and NCEP for the $\zeta_{-2.5}$ systems (Fig. 6b) that exceed the defined thresholds (±3 and ±5 systems) are smaller than in the $\zeta_{-1.5}$ (Fig. 6a). This result was expected because the systems with $\zeta_{-2.5}$ are included in $\zeta_{-1.5}$.

It is also important to point out that almost all the difference between RegCM3 and NCEP in the year of 1996 (Fig. 3a) is because of June (Figs. 5b, 6a, b) where the RegCM3 underestimated about 15 cyclones (Fig. 6a, b). During this month, for $\zeta_{-2.5}$, the NCEP presents 25 cyclogenesis being 12.8 its the climatology while the

Table 2 Number of months in that the difference (RegCM3-NCEP) was higher than the thresholds of the ±3 and ±5 systems

	$\zeta \leq -1.5 \times 10^{-5}$ s^{-1}	$\zeta \leq -2.5 \times 10^{-5}$ s^{-1}
Dif < −3	28 (23.3%)	23 (19.2%)
Dif > 3	28 (23.3%)	10 (8.3%)
Dif < −5	18 (15.0%)	8 (6.7%)
Dif > 5	13 (10.8%)	2 (1.7%)

Values in parenthesis are the differences in percentage

RegCM3 produced ten systems which is close to the climatology (see Fig. 3b). A detailed analysis of the mean vorticity field in June 1996 shows that the RegCM3 simulated a larger number of systems which left the analysis

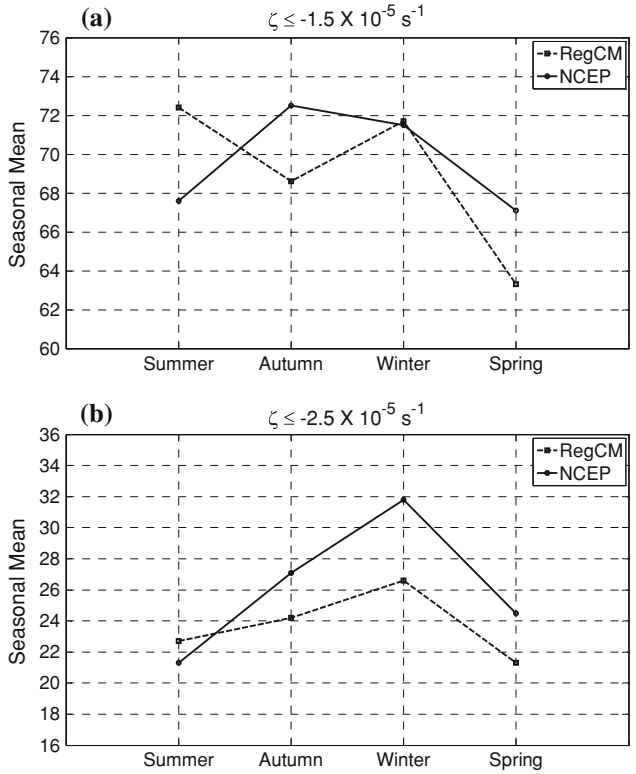

Fig. 7 Seazonal mean cyclogeneses detected in the NCEP (*full line*) and RegCM3 (*dotted line*) with initial vorticity **a** $\zeta \leq -1.5 \times 10^{-5}$ s^{-1} and **b** $\zeta \leq -2.5 \times 10^{-5}$ s^{-1}

region before they completed 24 h and, therefore they were not counted. Also, the RegCM3 presented lower number of multiple cyclonic vortices (similar to Fig. 2) than NCEP in this month.

3.4 Seasonal means

The cyclogenesis seasonal means using different vorticity thresholds are presented in Fig. 7. For $\zeta_{-1.5}$ (Fig. 7a), the NCEP (RegCM3) shows higher cyclogenetic activity during the autumn (summer) followed by winter (winter). In both, RegCM3 and NCEP, the minimum of cyclogenesis is found in spring. In the summer the cyclogenesis produced by the RegCM3 overcome those from NCEP due to the contribution of January and December months as shown in Fig. 5a, when all systems ($\zeta_{-1.5}$) are considered. This figure also shows that the smaller number of systems from the RegCM3 in March and May is responsible for smaller frequency of events in autumn compared to the NCEP. The RegCM3 bias is very small in each of the seasons, reaching a maximum of +7.1% in the summer.

Eliminating the initially weak systems from the climatology, the RegCM3 and NCEP present similar seasonal variation, with maximum of cyclogenesis during the winter (Fig. 7b). Also, the larger RegCM3 relative error occurs during winter, when the model underestimates 16.3% the initially intense cyclogenesis. However, in the summer RegCM3 overestimates is 6.6%.

The cyclogenesis seasonal variation with $\zeta_{-2.5}$ in the NCEP over the SAO (Fig. 7b) is similar to those obtained by Gan and Rao (1991) for South America and South Atlantic where there is a maximum in the winter and a minimum in the summer. For all systems ($\zeta_{-1.5}$) the seasonal distribution of NCEP (Fig. 7a) is similar to that obtained by Sinclair (1996) that identified small variations in the number of cyclogenesis during the year. However, when specific regions of the SAO are considered the season with higher cyclogenetic activity shows differences, as it will be discussed.

To identify the more favorable geographic regions for cyclogenesis occurrence, the spatial distribution of the seasonal density (total from 1990 to 1999) of cyclogenesis is presented in Figs. 8 and 9.

The inspection of Fig. 8a–d reveals three well defined cyclogenetic areas near the east coast of South America for the $\zeta_{-1.5}$ systems in the NCEP data: the southeastern coast of Argentina, near 48°S, with large density during the summer; (b) Uruguay, in the region of the La Prata River discharge, ~35°S, where the large density occurs in the spring, and (c) south/southeastern coast of Brazil, between 30° and 25°S, with maximum density in the summer. These three cyclogenetic cores have also been found in previous studies (Necco 1982a, b; Sinclair 1996; Hoskins and Hodges 2005; and Reboita et al. 2005).

There are some hypotheses for the existence of the cyclogenetic areas showed in Fig. 8. According to Gan and Rao (1991) and Sinclair (1996) the larger cyclogenesis occurrence in the southeastern Argentina (RG3) is associated with the baroclinic instability in the westerlies. Necco (1982a) mentioned that the upper level mobile troughs moving from the Pacific to the Atlantic Ocean are important feature for these cyclogenesis and Reboita (2008) confirmed it. The contribution of lee effect due to the Andes in ~48°S is pointed by Sinclair (1995) and Hoskins and Hodges (2005) as another important mechanism for the cyclones development. The influence of the mobile upper level troughs is also a mechanism considered very important for cyclogenesis over Uruguay (RG2) and its surrounding areas (Taljaard 1967; Necco 1982b; Seluchi 1995; Seluchi et al. 2001; Vera et al. 2002; Reboita 2008). Moreover, the Andes Mountains effect in the westerlies contributes to cyclogeneses (Gan and Rao 1994). The mountains induce a topographic wave with the trough located near to the Uruguay and south of Brazil (Satyamurty et al. 1980; Lenters and Cook 1997). Associated to these troughs (transient and semi-stationary), there is moisture transport from Amazon basin to the La Plata basin at low levels which is related to the low level jet eastern of the Andes, contributing for the development of the cyclone systems in this region (Sinclair 1996; Vera et al. 2002;

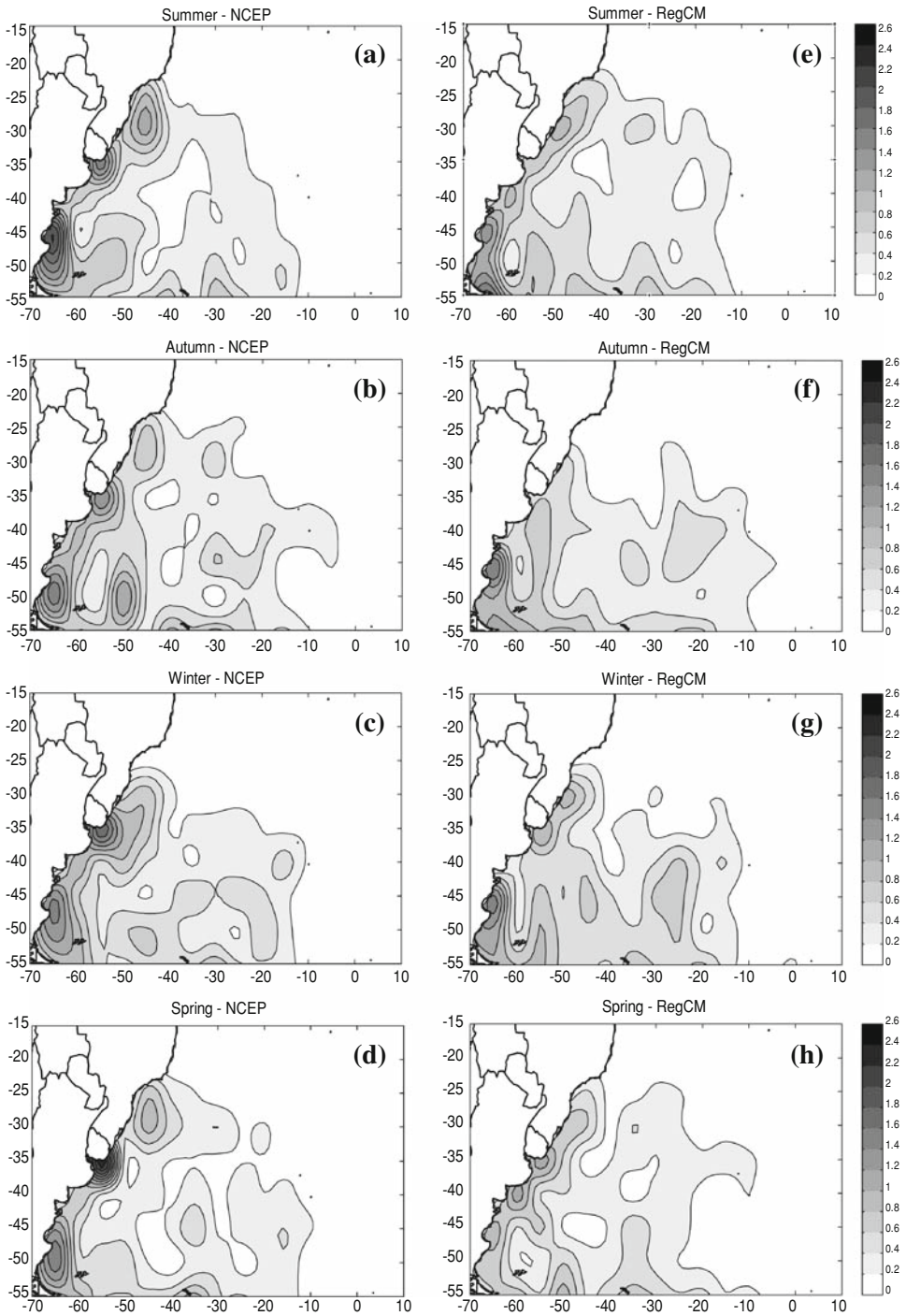

Fig. 8 Seasonal density of the cyclogeneses for $\zeta \leq -1.5 \times 10^{-5}\ s^{-1}$ in the NCEP (*left*) and RegCM3 (*right*). Density (number of systems per km^2) has to be multiplied by 10^4. In the *shaded scale* the value 1 corresponds to approximately 25 systems

Reboita 2008). However, this jet is sometimes directed to the south/southeast of Brazil favoring the cyclogenesis on the Brazilian coast (RG1). The upper level subtropical jet can also influence these cyclogenesis (Hoskins and Hodges 2005) as well as the air–sea processes interactions through latent and sensible heat transfer (Sinclair 1995; Vera et al. 2002; Reboita 2008; Iwabe and da Rocha 2009) in RG1.

Comparing the cyclogenesis density simulated (Fig. 8e–h) with the NCEP (Fig. 8a–d) it can be noted that the RegCM3 was able to reproduce the main aspects of these fields. However, it is observed that the model generally underestimates the density. In particular, the RegCM3 always simulates less cyclogenesis density in the eastern Uruguay (RG2).

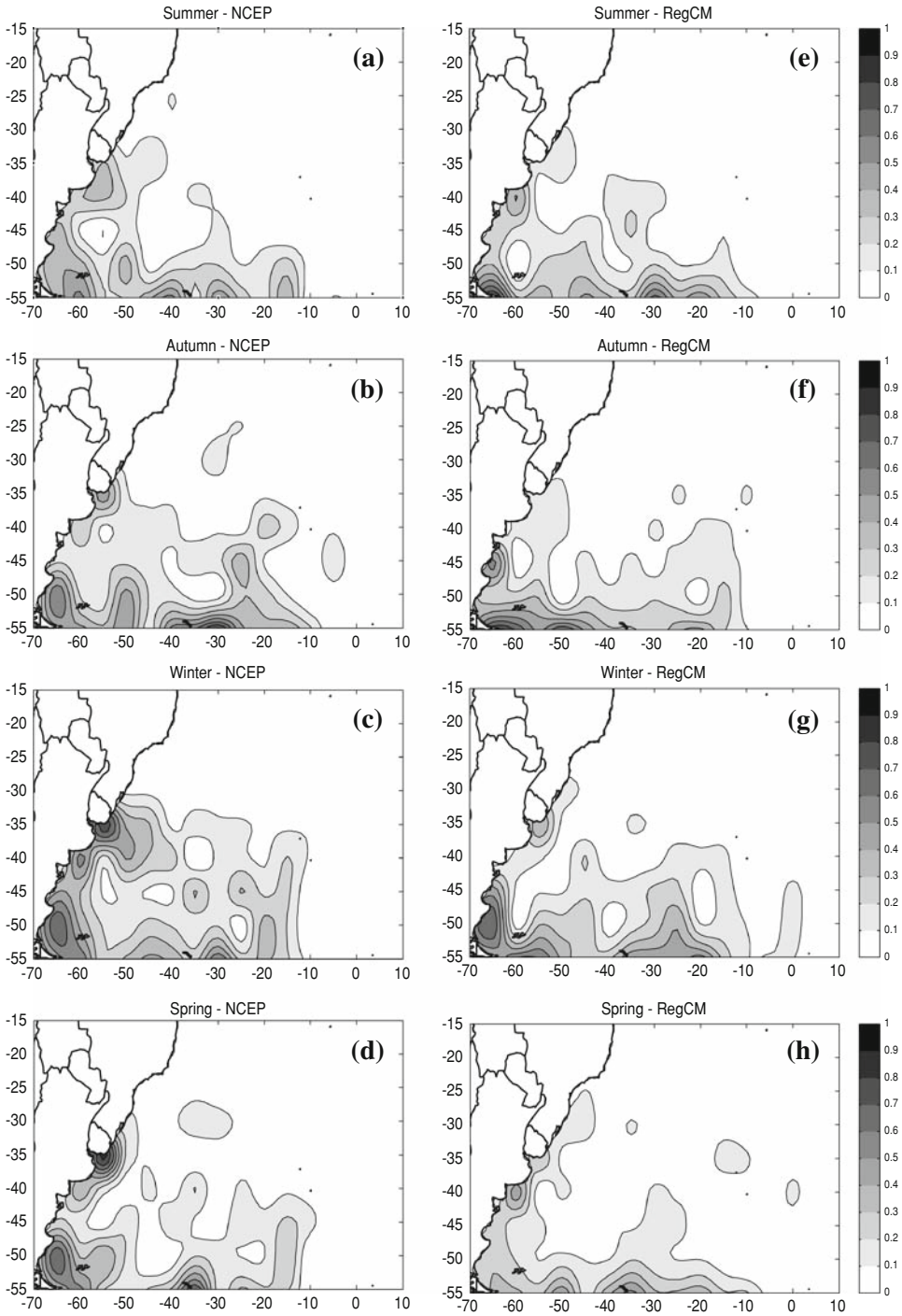

Fig. 9 Similar to Fig. 8 but for $\zeta \leq -2.5 \times 10^{-5}\ s^{-1}$. In the *shaded scale* the value 0.5 corresponds to approximately 12.5 systems

Similar to the NCEP (Fig. 8a), the RegCM3 (Fig. 8e) also shows larger cyclogenesis density over the south/southeastern coast of Brazil (RG1) during the summer, but it underestimates the density and its core maximum is displaced toward southwestern (Fig. 8a–e). However, during the winter (Fig. 8c–g) and spring (Fig. 8d–h) the simulated density is similar to the NCEP. In the Uruguay coast (RG2), the RegCM3 does not reproduce the density maximum presents in the NCEP during the summer (Fig. 8a–e) and autumn (Fig. 8b–f), but it simulates a weaker maximum in the winter (Fig. 8c–g) and spring (Fig. 8d–h).

In the southeastern coast of Argentina (RG3), during the summer (Fig. 8a–e) and autumn (Fig. 8b–f) the model simulates two main centers of cyclogenesis: one between 50° and 45°S and other in the southern boundary of the

domain (55°S). This result differs from the NCEP which only shows a core that oscillates between 45°S (summer) and 50°S (autumn). During the winter (Fig. 8c–g), the RegCM3 reproduces the intensity and location of the cyclogenetic core obtained in the NCEP. In the RG3, the model underestimates the cyclogenesis density in the spring (Fig. 8d–h). The simulated cyclogenesis maximum density in the RG3 occurs in the autumn and winter, differing from the NCEP where the maximum is only in the summer.

When only the $\zeta_{-2.5}$ systems are considered, there is a clear reduction of the cyclogenetic density in the south/southeastern Brazilian coast for the NCEP and RegCM3 (Fig. 9). This reduces the number of cyclogeneses areas near the east coast of South America to two and the larger cyclogenetic activity occurs in the winter (Fig. 9c–g).

Close to the La Prata River discharge (RG2) the NCEP shows intense cyclonegesis during all seasons with higher density during the spring (Fig. 9d). However, similar to Fig. 8, the area occupied is larger in the winter (Fig. 9c) which may explain the larger number of cyclogenesis in this season (Fig. 7b) when the cyclogenetic density is integrated over all RG2. On the other hand, the RegCM3 shows reduced cyclogenetic activity in the coast of Uruguay being displaced southward during the summer (Fig. 9a, b) and spring (Fig. 9d–h). The simulated cyclogenetic density area over southeastern Argentina (RG3) is also displaced southward, except in the winter (Fig. 9c–g), where the cyclogenetic cores are similar in position to the NCEP.

3.5 The three cyclogenetic regions: seasonal variability

Figures 8 and 9 clearly show that there are three regions where the cyclogenesis is more frequent in the east coast of South America. However, the density of the cyclogenesis is dependent of the region and season. In order to investigate theses questions three subdomains (RG1, RG2 and RG3) were established as shown in Fig. 1.

The total number of systems from 1990 to 1999 in the RG1, RG2 and RG3 are presented in Table 3. In general, the total number of systems in each area is larger in the NCEP than RegCM3. Concerning the cyclogenesis initiated with $\zeta_{-1.5}$, the larger RegCM3 underestimation is obtained in the RG1 (−24%), while the better agreement between RegCM3 and NCEP occurs in the RG3 (−6%). For the initially more intense systems the RegCM3 was less skilful in the RG2, where there is a negative relative bias of −47%. In the RG1 as well as in the RG3 the numbers of the initially more intense cyclogenesis simulated are very similar to the NCEP.

As will be discussed in the Sect. 3.6, the RegCM3 simulated systems are weaker than in the NCEP. This implied that in many simulated systems the vorticity threshold ($\zeta_{-1.5}$) to tracking is not reached, being more common in RG1 and RG2. In these regions, a reason for the RegCM3 cyclogenesis underestimation is that the simulated mid-high levels transient troughs (which cross the South America from Pacific Ocean at subtropical latitudes) are weaker than in the NCEP. Other feature that contributes for weaker systems in model is that RegCM3 underestimation of the low-level moisture transport from tropics to subtropics (Fernandez et al. 2006; Reboita 2008). As previously presented in the literature, mid-high levels trough (Seluchi 1995; Vera et al. 2002; Reboita 2008) and moisture availablity (Vera et al. 2002; Reboita 2008) are important mechanisms for cyclone development in the RG1 and RG2. In the RG3 the RegCM3 simulates better the mid-high levels trough amplitude, explaining the better agreement between RegCM3 and NCEP cyclones climatology.

The rate between initially intense and all systems simulated by RegCM3 is similar to that obtained with the NCEP (Table 3), except for the RG2 where it is almost half of the NCEP. In RG1, the RegCM3 and NCEP indicate predominance of initially weak cyclones, and the initially more intense events represents 14 and 12%, respectively, of the total cyclogenesis.

For regions RG1, RG2 and RG3, the cyclogenesis seasonal means and their standard deviation are presented in Figs. 10 and 11, respectively. Figure 10 shows that the cyclonegenis annual cycle in each of these regions is not the same than over the SAO (Fig. 7a). The larger differences between RegCM3 and NCEP occur in the RG2

Table 3 Total number of cyclogeneses from 1990 to 1999 that initiated in the three cyclogenetic regions (RG1, RG2 and RG3) and the ratio $\zeta_{-2.5}/\zeta_{-1.5}$ in percentage

Cyclogenetic regions	$\zeta \leq -1.5 \times 10^{-5}\ s^{-1}$		$\zeta \leq -2.5 \times 10^{-5}\ s^{-1}$		$(\zeta_{-2.5}/\zeta_{-1.5}) \times 100$	
	RegCM3	NCEP	RegCM3	NCEP	RegCM3	NCEP
RG1	225 (76%)	296	32 (84%)	38	14%	12%
RG2	276 (85%)	325	72 (53%)	135	26%	41%
RG3	390 (94%)	417	150 (100%)	150	38%	36%

Values in parenthesis are the ratio RegCM3/NCEP in percentage

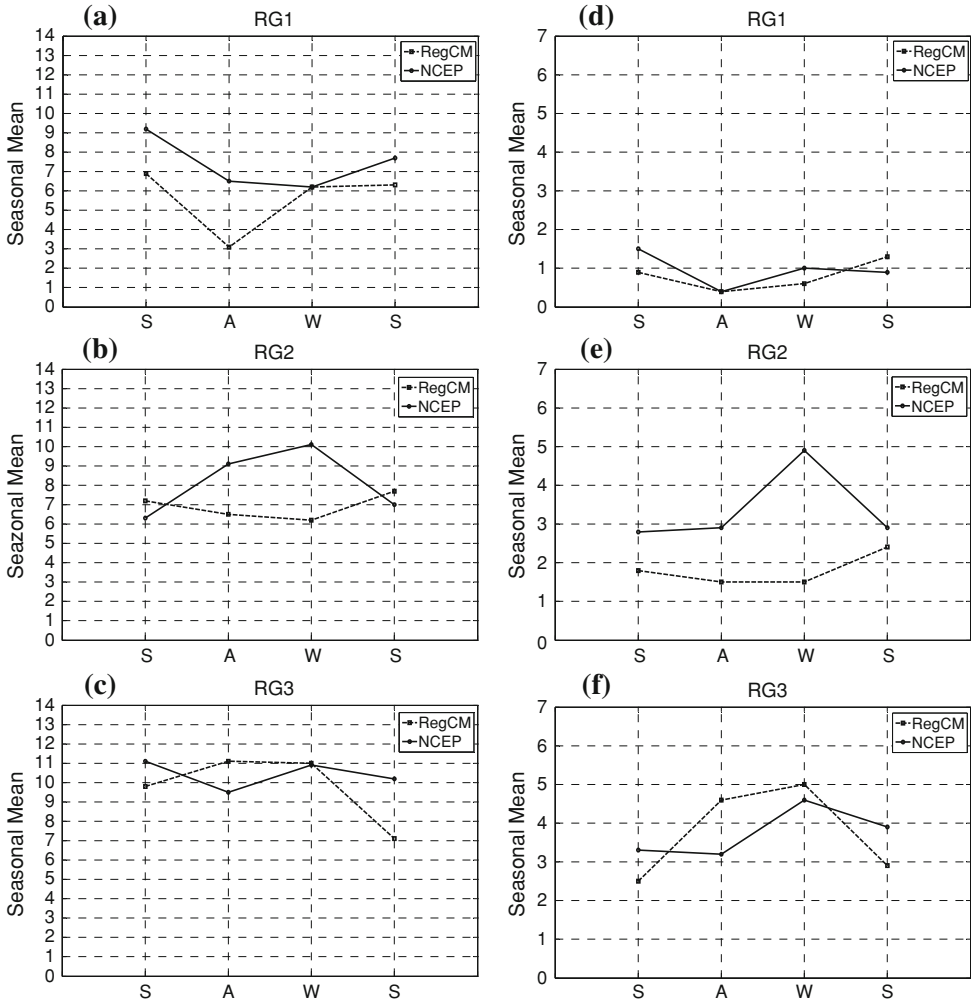

Fig. 10 Seasonal mean of the cyclogeneses detected in the NCEP (*full line*) and RegCM3 (*dotted line*) with initial vorticity of $\zeta \leq -1.5 \times 10^{-5}$ s^{-1} (*left*) and $\zeta \leq -2.5 \times 10^{-5}$ s^{-1} (*right*) in each cyclogenetic region shown in Fig. 1. In the horizontal axis the season order is summer (S), autumn (A), winter (W) and spring (S)

(Fig. 10b–e). In this area, the RegCM3 (Fig. 10b–e) simulates an almost uniform distribution of the cyclogenesis during the year while the NCEP (Fig. 10b–e) shows a peak in the winter. For the RG1 (Fig. 10a) NCEP and RegCM3 present larger frequency of $\zeta_{-1.5}$ during the summer and suffer a reduction in the autumn, and the RegCM3 in general underestimates the NCEP. In this same area, the $\zeta_{-2.5}$ are well distributed during the year (Fig. 10d) and they represent a small fraction of the total (Fig. 10a–c). In RG3 (Fig. 10c), except by the drastic reduction of the simulated $\zeta_{-1.5}$ cyclonegenesis during the spring (Fig. 10c), the RegCM3 annual cycle is similar to the NCEP. For the more intense cyclogenesis (Fig. 10f) the amplitude of annual cycle is larger and there is a peak in the winter and a decrease in the summer.

In general, considering the three areas and the two different vorticity thresholds, the interanual variability, as measured by the standard deviation, simulated by the RegCM3 is similar to the NCEP (Fig. 11), somewhat centered in different mean values (Fig. 10). The large interannual variability in the NCEP and RegCM3 depends of the region. The standard deviation indicates that the interannual variability over the RG1 is smaller than in the RG2 and RG3 (Fig. 11). Moreover, in this region, the standard deviation of the RegCM3 and NCEP are similar, around 2 (1) for all (more intense) systems. The NCEP shows larger interannual variability during winter in the RG3 (Fig. 11c) and the RegCM3 is not able to simulate this variability. In this area, the RegCM3 presents better agreement with NCEP for the $\zeta_{-2.5}$ intense cyclones (Fig. 11f).

3.6 Mean characteristics of the NCEP and RegCM3 cyclogenesis

The mean characteristics, from 1990 to 1999, of the cyclones detected in the SAO are presented through relative frequency distributions of some parameters in Figs. 12 and 13. The simulated cyclogenesis, in general, are weaker than that in the NCEP, for both the initial vorticity (Fig. 12a) as for the mean vorticity during their lifetime (Fig. 12b). It is worthy to mention that from a qualitative

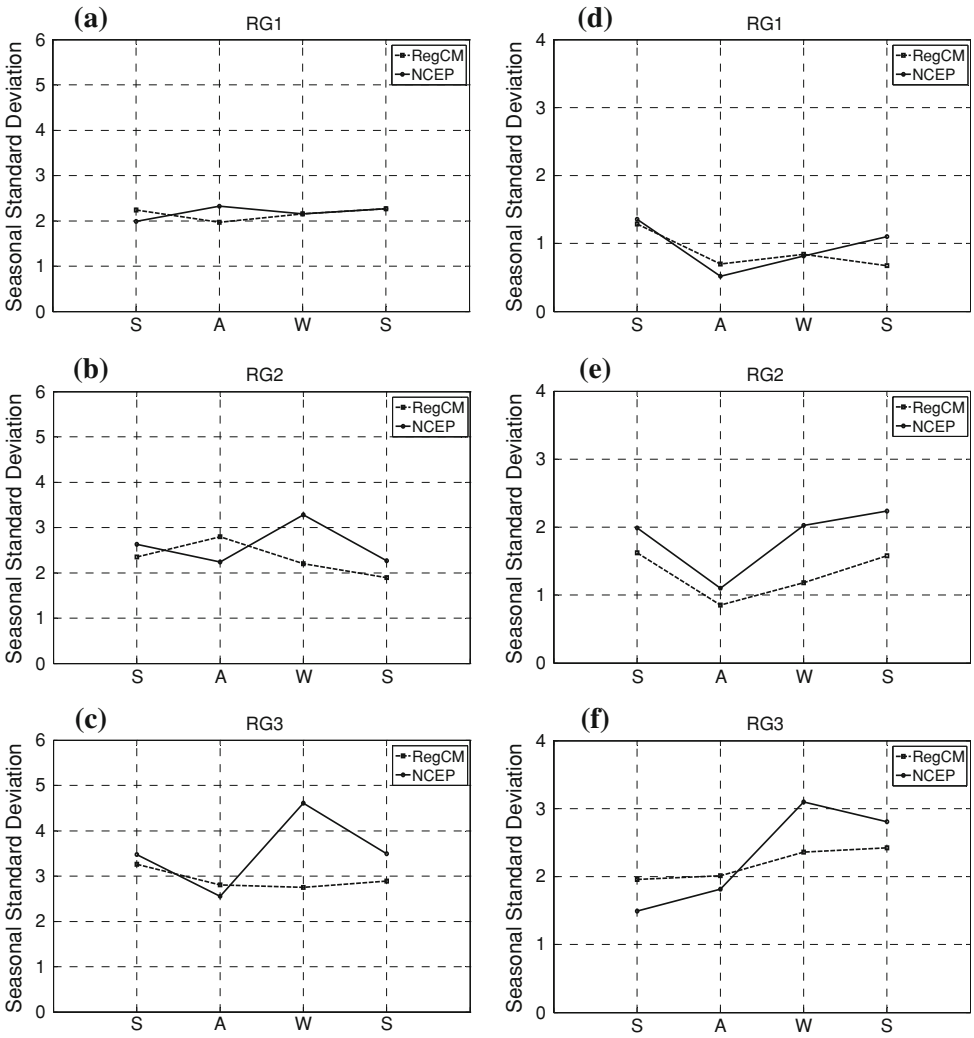

Fig. 11 Similar to Fig. 10, but for the seasonal standard-deviation

analysis of the vorticity field it was noted that the simulated systems initiate on average 12–24 h after the NCEP. However, they usually decay afterwards. Due to these features, the simulated cyclones have a lifetime frequency distribution similar to the NCEP (Figs. 12c, 13c).

The differences in the shape of the frequency distributions between the RegCM3 and NCEP for the mean traveled distance (Figs. 12d, 13d) and mean velocity (Figs. 12e, 13e) are smaller for the initially weak than for intense systems. Considering the cyclones that initiated with $\zeta_{-1.5}$ and $\zeta_{-2.5}$ the RegCM3 and NCEP show that there are a higher relative number of systems with mean vorticity between -3.5 and -2.0×10^{-5} s^{-1}, lifetime of 1–2 days, which travel a distance of 1,500–2,000 km, and having an average velocity of 10–15 m s^{-1}. The similarity of the mean values and histograms permit to conclude that the RegCM3 simulates the main climatological characteristics of the cyclones in the SAO when compared to the NCEP.

4 Summary and conclusions

The main cyclogenesis climatological features simulated by the RegCM3 over the SAO during 1990 to 1999 were analyzed in this work. A numerical scheme was used to tracking the cyclones with minimum lifetime of 24 h and initial cyclonic relative vorticity threshold of -1.5×10^{-5} s^{-1} ($\zeta_{-1.5}$) and -2.5×10^{-5} s^{-1} ($\zeta_{-2.5}$). The numerical results were compared with the NCEP reanalysis.

During the 1990−1999 period were identified 2,760 and 2,787 cyclogenesis in the RegCM3 and NCEP, respectively, which correspond to an annual mean of 276.0 ± 11.2 and 278.7 ± 11.1. These values indicate a small underestimation (−1%) by the RegCM3 in comparison with the NCEP total cyclogenesis over SAO and a good representation of the interannual variability, as measured by the standard deviation. The model underestimation increases when one considers the initially more intense

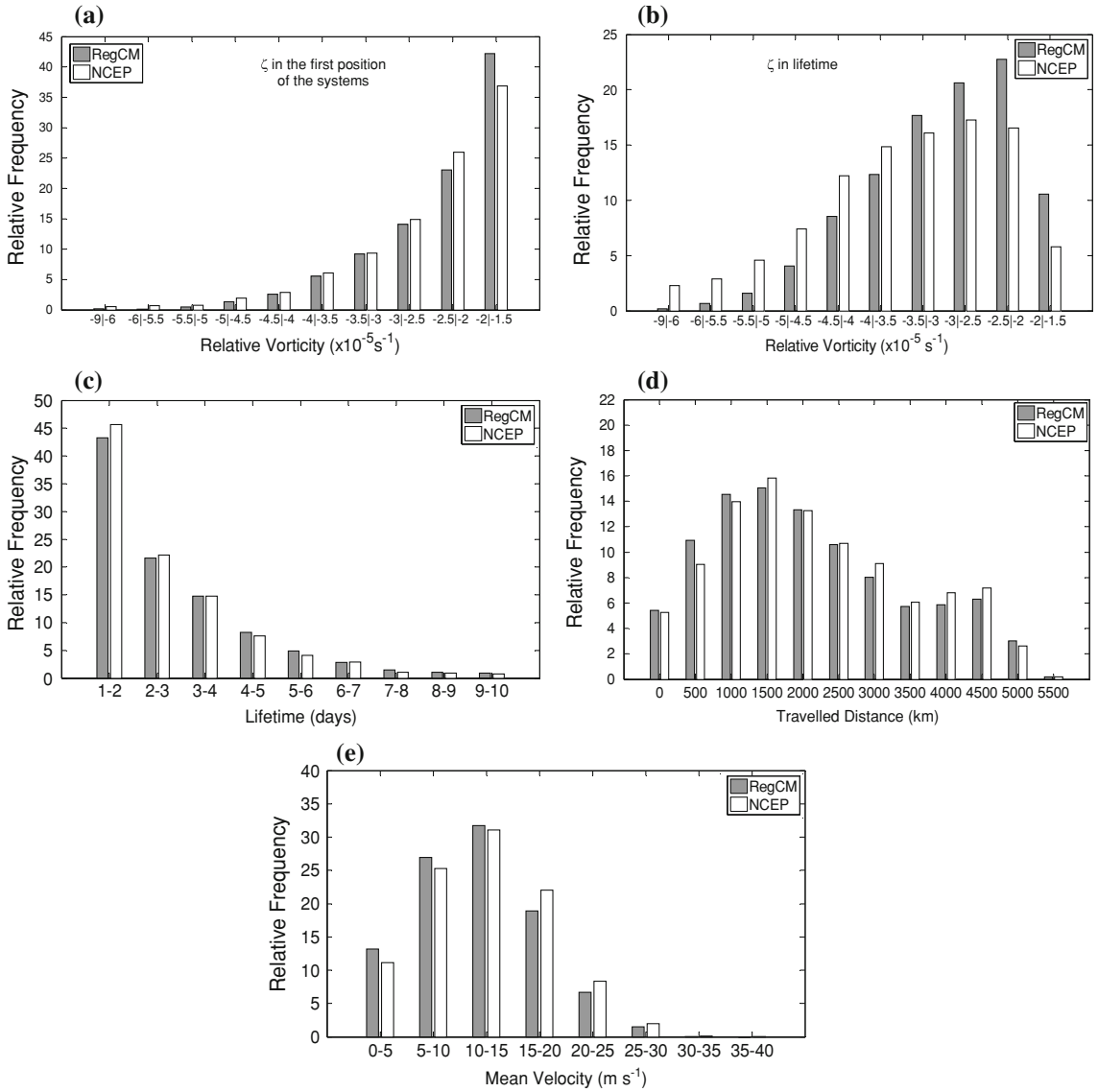

Fig. 12 Histograms for the $\zeta \leq -1.5 \times 10^{-5}$ s^{-1} systems of the **a** vorticity in the first cyclone position, **b** their lifetime, **d** distance travelled and **e** mean velocity obtained from the NCEP (*white bars*) and RegCM3 (*gray bars*)

cyclones. For example, for the cyclonic vorticity threshold of -2.5×10^{-5} s^{-1} the RegCM3 simulates 948 systems, while the NCEP presents 1,047 events, implying in a RegCM3 negative relative bias of 9.5%.

It was demonstrated that the annual cycle of cyclogenesis over the SAO is dependent of the initial intensity of the systems. For all systems ($\zeta_{-1.5}$) the annual cycle is not well defined, i.e., the monthly difference of the number of cyclogenesis is small which agrees with Sinclair (1996). The initially $\zeta_{-2.5}$ cyclogenesis in NCEP and RegCM3 show a well defined annual cycle, as in Gan and Rao (1991), with higher and lower frequencies in winter and summer months, respectively.

Three selected regions of cyclones development also indicated the importance of the initial intensity. Applying the initial $\zeta_{-1.5}$ threshold, three main cyclogenetic areas were emphasized in the east coast of South America: southeastern coast of Argentina, ~48°S; the La Prata river discharge in Uruguay, ~35°S; and the south/southeastern coast of Brazil. The RegCM3 was able to simulate these three cylogenesis regions, however in some cases (mainly in RG1 and RG2) it underestimates or misplace the cyclogenesis density areas. These differences are probably due to the RegCM3 deficiencies in the simulation of mid-high levels transient troughs and low-level moisture transport. For the $\zeta_{-2.5}$, the cyclogenetic core in the south/southeastern coast of Brazil disappears in the NCEP and RegCM3. This result is similar to previous studies that used sea level pressure to identify cyclogenesis (Gan and Rao 1991) and it suggests that the

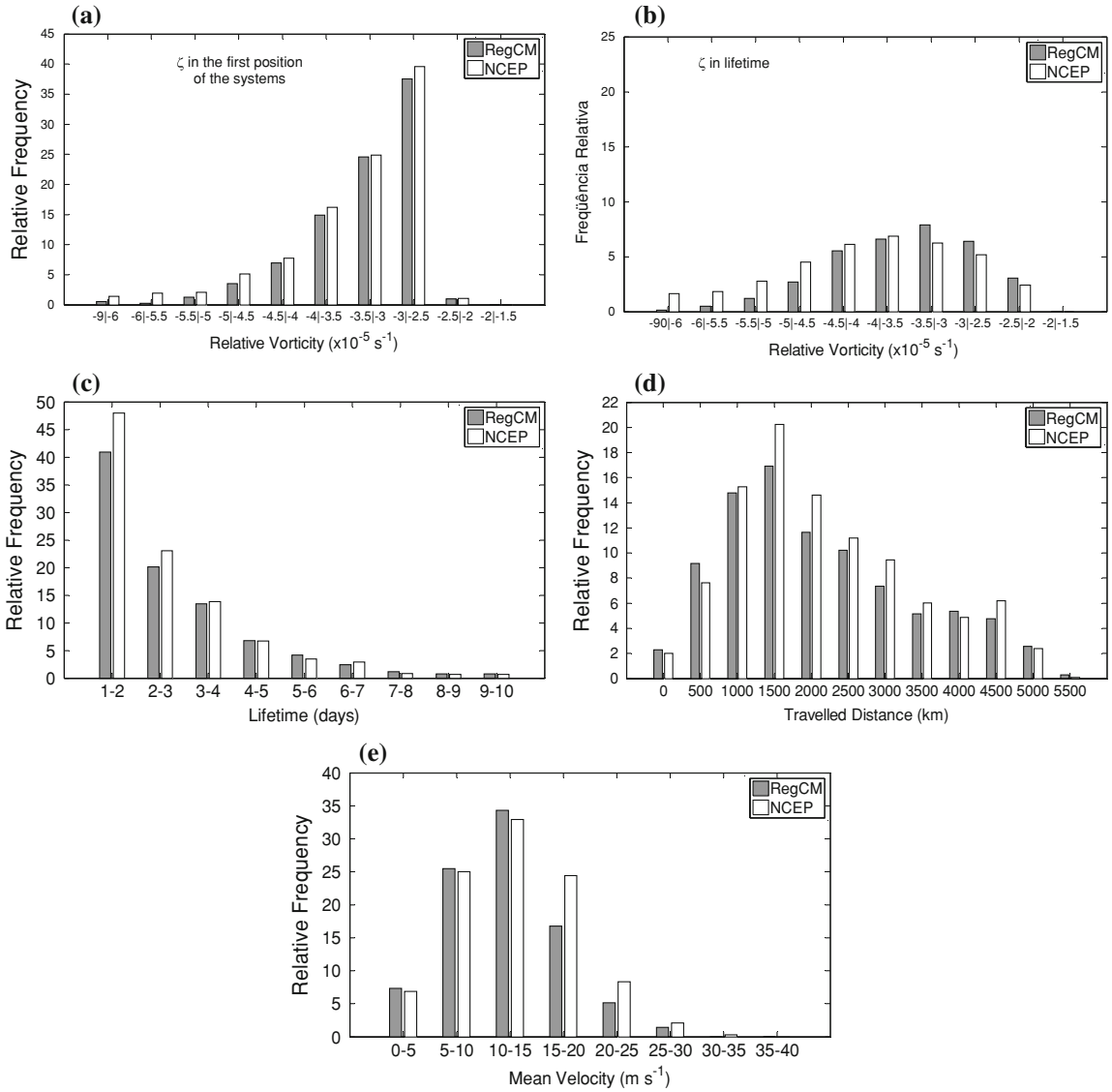

Fig. 13 Similar to Fig. 13 but for the systems with $\zeta \leq -2.5 \times 10^{-5}$ s^{-1}

vorticity methodology is important to identify less intense systems.

The season of higher frequency for cyclogenesis ($\zeta_{-1.5}$) on specific regions is different when the whole SAO is considered. The NCEP and RegCM3 present more cyclogenesis during the summer in the south/southeastern coast of Brazil, which agrees with Sinclair (1996). In the La Prata River discharge (RG2) NCEP shows a peak in the winter, which is in agreement with Gan and Rao (1991) and Sinclair (1996), but the RegCM3 has a maximum in the spring. In the NCEP, the larger frequency in winter can be explained by the interaction between mid-level troughs and larger low-levels temperature gradient. However, in the RegCM3 these features are similar in both seasons, but the model simulates larger moisture transport during the spring, which could help to understand the seasonality differences (Reboita 2008). On the southeast coast of Argentina the NCEP shows more frequent cyclogenesis during the summer, while the RegCM3 simulates a uniform distribution along the year. In this area, the difference can be related to the proximity of the southern boundary of the domain, where the model tends to displace the cyclogenetic maximum to the south of the RG3.

Considering the entire SAO, the main cyclogenesis features such as the mean initial cyclonic vorticity (-2.5×10^{-5} s^{-1} for NCEP and -2.4×10^{-5} s^{-1} for RegCM3), lifetime (2.6 days for NCEP and 2.7 days for RegCM3), traveled distance (2,437 km for NCEP and 2,377 for RegCM3), and mean speed (11.0 m s^{-1} for NCEP and 10.5 m s^{-1} for RegCM3) was well simulated by

the RegCM3. These results indicate that the RegCM3 is able to simulate the main features of the cyclogenesis climatology on the SAO and it may be very useful to investigate many other properties of the cyclones development in the region.

Acknowledgments The authors would like to thank FAPESP (processes 04/02446-7 and 01/13925-5) and the CNPq (processes 475281/2003-9, 300348/2005-3, and 476361/2006-0) for financial support. We also acknowledge the ICTP for providing the RegCM3 and NCEP for the reanalysis. CAPES has also provided partial support for this research.

References

Anthes RA (1977) A cumulus parameterization scheme utilizing a one-dimensional cloud model. Mon Weather Rev 117:1423–1438

Blender R, Fraedrich K, Lunkeit F (1997) Identification of cyclone-track regimes in the North Atlantic. Q J R Meteorol Soc 123:727–741

Cressman GP (1959) An operational objective analysis system. Mon Weather Rev 7(10):367–374

Dickinson RE, Errico RM, Giorgi F, Bates GT (1989) A regional climate model for the western United States. Clim Change 15:383–422

Dickinson RE, Henderson-Sellers A, Kennedy PJ (1993) Biosphere–Atmosphere Transfer Scheme (BATS) version 1E as coupled to the NCAR Community Climate Model. Tech. Rep. TN-387 + STR. NCAR, Boulder, Colorado, p 72

Emanuel KA (1991) A scheme for representing cumulus convection in large-scale models. J Atmos Sci 48:2313–2335

Fernandez JPR, Franchito SH, Rao VB (2006) Simulation of the summer circulation over South America by two regional climate models. Part I: Mean climatology. Theor Appl Climatol 86:247–260

Fyfe JC (2003) Extratropical Southern Hemisphere cyclone: Harbingers of climate change? J Clim 16:2802–2805

Gan MA, Rao VB (1991) Surface cyclogenesis over South America. Mon Weather Rev 119:293–302

Gan MA, Rao VB (1994) The influence of the Andes Cordillera on transient disturbances. Mon Weather Rev 122:1141–1157

Giorgi F (1990) Simulation of regional climate using a limited area model nested in a general circulation model. J Clim 3(9):941–963

Giorgi F (1991) Sensitivity of simulated summertime precipitation over the western United States to physics parameterizations. Mon Weather Rev 119:2870–2888

Giorgi F, Mearns LO (1991) Approaches to the simulation of regional climate change: a review. Rev Geophys 29(2):191–219

Grell GA (1993) Prognostic evaluation of assumptions used by cumulus parameterizations. Mon Weather Rev 121:764–787

Hodges KI (1994) A general method for tracking analysis and its application to meteorological data. Mon Weather Rev 122:2573–2586

Hodges KI (1996) Spherical nonparametric estimators applied to the UGAMP model integration for AMIP. Mon Weather Rev 124:2914–2932

Holtslag AAM, de Bruijn EIF, Pan HL (1990) A high resolution air mass transformation model for short-range weather and forecasting. Mon Weather Rev 118:1561–1575

Hoskins BJ, Hodges KI (2005) A new perspective on southern hemisphere storm tracks. J Clim 18:4108–4129

Hudson DA (1997) Southern African climate change simulated by the GENESIS GCM. S Afr J Sci 93:389–408

Hudson DA, Hewitson BC (1997) Mid-latitude cyclones south of Africa in the GENESIS GCM. Int J Climatol 17:459–473

Intergovernmental Panel on Climate Change—IPCC (2007) Climate change 2007: the physical science basis. Cambridge University Press, Cambridge, 989 pp

Iwabe CN, da Rocha RP (2009) An event of stratospheric air intrusion and its associated secondary surface cyclogenesis over the South Atlantic Ocean. J Geophys Res 114:D09101. doi:10.1029/2008JD011119

Kalnay E et al (1996) The NCEP/NCAR 40-Year Reanalysis Project. Bull Am Meteorol Soc 77:437–471 Coauthors

Kanamitsu M, Ebisuzaki W, Woollen J, Yang S-K, Hnilo JJ, Fiorino M, Potter GL (2002) NCEP-DOE AMIP-II Reanalysis (R-2). Bull Am Meteorol Soc 83:1631–1643

Kiehl JT, Hack JJ, Bonan GB, Boville BA, Briegleb BP, Williamson DL, Rasch PJ (1996) Description of the NCAR Community Climate Model (CCM3), Tech. Rep. TN-420 + STR, NCAR, Boulder, Colorado, 152 pp

König W, Sausen R, Sielmann F (1993) Objective identication of cyclones in GCM simulations. J Clim 6:2217–2231

Lambert SJ (1988) A cyclone climatology of the Canadian Centre General Circulation Model. J Clim 1:109–115

Lambert SJ (1995) The effect of enhanced greenhouse warming on winter cyclone frequencies and strengths. J Clim 8:1447–1452

Lenters JD, Cook KH (1997) On the origin of the Bolivian high and related circulation features of the South American climate. J Atmos Sci 54:656–677

Lionello P, Boldrin U, Giogi F (2008) Future changes in cyclone climatology over Europe as inferred from a regional climate simulation. Clim Dyn 30:657–671

Loveland TR, Reed BC, Brown JF, Ohlen DO, Zhu J, Yang L, Merchant JW (2000) Development of a global land cover characteristics database and IGBP DISCOVER from 1-km AVHRR Data. Int J Remote Sens 21:1303–1330

Murray RJ, Simmonds I (1991) A numerical scheme for tracking cyclone centers from digital data. Part II: Application to January and July general circulation model simulations. Aust Meteor Mag 39:167–180

Necco GV (1982a) Comportamiento de Vortices Ciclonicos En El Area Sudamerica Durante El FGGE: cyclogenesis. Meteorologica 13(1):7–19

Necco GV (1982b) Comportamiento de Vortices Ciclonicos En El Area Sudamerica Durante El FGGE: Trayectorias y Desarrollos. Meteorologica 13(1):21–34

Pal JS, Small EE, Elthair EA (2000) Simulation of regional-scale water and energy budgets: representation of subgrid cloud and precipitation processes within RegCM. J Geophys Res 105:29579–29594

Pal JS et al (2007) The ITCP RegCM3 and RegCNET: Regional Climate Modeling for the Developing World. Bull Am Meteorol Soc 88(9):1395–1409 Coauthors

Palmén E, Newton CW (1969) Atmospheric circulation systems: their structure and physical interpretation. Academic Press, New York 603 p

Peixoto JP, Oort AH (1992) Physics of climate. American Institute of Physics, 520 pp

Pinto JG, Spangehl T, Ulbrich U, Speth P (2006) Sensitivities of a cyclone detection and tracking algorithm: individual tracks and climatology. Meteorol Zeitschrift 14:823–838

Raible CC, Blender R (2004) Northern Hemisphere midlatitude cyclone variability in GCM simulations with different ocean representations. Clim Dyn 22:239–248

Reboita MS (2008) Ciclones Extratropicais sobre o Atlântico Sul: Simulação Climática e Experimentos de Sensibilidade. Ph.D.

thesis in meteorology. Department of Atmospheric Sciences, São Paulo University. Available in http://www.dca.iag.usp.br/www/teses/2008/

Reboita MS, da Rocha RP, Ambrizzi T (2005) Climatologia de Ciclones sobre o Atlântico Sul Utilizando Métodos Objetivos na Detecção destes Sistemas (in Portuguese). In: Proceedings of 9th Argentian Congress, Buenos Aires

Reynolds RW, Rayner NA, Smith TM, Stokes DC, Wang W (2002) An improved in situ and satellite SST analysis for climate. J Clim 15:1609–1625

Satyamurty P, Santos RP, Lems MAM (1980) On the stationary trough generated by the Andes. Mon Weather Rev 108:510–520

Satyamurty P, Ferreira CC, Gan MA (1990) Cyclonic vortices over South América. Tellus 42A:194–201

Seluchi M (1995) Diagnóstic Y Prognóstico de Situaciones Sinópticas Conducentes a Ciclogénesis sobre el Este de Sudamérica. Geofísica Int 34(2):171–186

Seluchi M, de Calbete NO, Rozante JR (2001) Análisis de Un Desarrollo Ciclónico en la Costa Oriental de América Del Sur. Rev Brasil Meteorol 16(1):51–65

Seth A, Rojas M (2003) Simulation and sensitivity in a nested modeling system for tropical South America. Part I: reanalysis boundary forcing. J Clim 16:2453–2467

Simmonds I, Keay K (2000) Variability of southern hemisphere extratropical cyclone behavior, 1958–1997. J Clim 13:550–561

Sinclair MR (1994) An objective cyclone climatology for the southern hemisphere. Mon Weather Rev 122:2239–2256

Sinclair MR (1995) A climatology of cyclogenesis for the southern hemisphere. Mon Weather Rev 123:1601–1619

Sinclair MR (1996) Reply. Mon Weather Rev 124:2615–2618

Sinclair MR (1997) Objective identification of cyclones and their circulation intensity, and climatology. Weather Forecast 12:595–612

Sinclair MR, Watterson IG (1999) Objective assessment of extratropical weather systems in simulated climates. J Clim 12:3467–3485

Sugahara S (2000) Variação Anual da Freqüência de Ciclones no Atlântico Sul. In: Proceedings of the 11th Brazilian Congress of Meteorology, 11, Rio de Janeiro

Taljaard JJ (1967) Development, distribution and movement of cyclones and anticyclones in the Southern Hemisphere during IGY. J Appl Meteorol 6:973–987

Uppala SM et al (2005) The ERA40 reanalysis. Q J R Meteorol Soc 131:2961–3012 Coauthors

Vera C, Vigliarolo PK, Berbery EH (2002) Cold Season synoptic-scale waves over subtropical South America. Mon Weather Rev 130:684–699

Watterson IG (2006) The intensity of precipitation during extratropical cyclones in global warming simulations: a link of cyclone intensity? Tellus 58A:82–97

Zeng X, Zhao M, Dickinson RE (1998) Intercomparison of Bulk Aerodynamic Algorithms for the computation of sea surface fluxes using TOGA COARE and TAO data. J Clim 11:2628–2644

Zhang Y, Wang WC (1997) Model-simulated northern winter cyclone and anticyclone activity under a greenhouse warming scenario. J Clim 10:1616–1634